COMPDYN 2015
5th ECCOMAS Thematic Conference on
Computational Methods in Structural Dynamics and Earthquake Engineering
M. Papadrakakis, V. Papadopoulos, V. Plevris (eds.)
Crete Island, Greece, 25–27 May 2015

AN ENHANCED COMPONENT BASED MODEL FOR STEEL LINKS IN HYBRID STRUCTURES: DEVELOPMENT, CALIBRATION AND EXPERIMENTAL VALIDATION

M. Manfredi[1], **F. Morelli** [1] **and W. Salvatore**[1]

[1] Department of Civil and Industrial Engineering - University of Pisa
largo Lucio Lazzarino 1, 56122, Pisa
martin.doc@hotmail.it, francesco.morelli@dic.unipi.it, walter@ing.unipi.it

Keywords: steel-concrete hybrid structures, steel structures, concrete shear walls, experimental test, dissipative systems, component-based model.

Abstract. *In the present paper the development, calibration and experimental validation of an enhanced component based model of a dissipative steel link connecting a reinforced concrete wall and a steel gravity frame is presented. The structural consists in an hybrid coupled shear wall (HCSW), developed within the INNOHYCO project (Dall'Asta et al., 2014), obtained coupling an RC wall with two side steel columns by means of steel links where the energy dissipation takes place. The experimental results carried on a subsystem representing a portion of the shear wall, the dissipative link and one side column, showed that the global dissipative behavior is strongly affected by the characteristics of the link-to-column connection. In particular the prestressing force of the seat angle connection bolts influence in a decisive way the dissipative capacity of the system, especially for the low amplitude cycle. For this reason, an experimental campaign on two different hybrid system containing the dissipative element and the aforementioned connections has been carried out. A non-linear cyclic component-based model of the entire sub-assemblage is then developed and calibrated on the base of experimental results.*

1 INTRODUCTION

During the last decades, several researches have been conducted in order to find structural solutions capable to resist to the seismic lateral loads, assuring the life safety in case of strong intensity earthquakes and minimizing the damages to structural and non structural elements in case of low-to-mid earthquakes. In order to reach these goals, particular attention has been given to dissipative structures that allows the realization of building characterized by relatively small element section, if compared to the structures designed to resist elastically to the seismic action, but with a comparable, if not even greater, safety level. Generally speaking, the optimal solutions should be so characterized by suitable stiffness, resistance, global and local ductility. In order to minimize the damages to the non structural elements and the gravity resisting system and, at the same time, to allow a fast recover after low-to-mid intensity earthquakes, the dissipation of energy should be localized in suitable elements easy to replace after the seismic event.

An effective structural solution capable of offering significant advantages in terms of resistance and lateral stiffness are composite constructions. They have been common in Europe and US for over half a century through the use of composite beam and joist floor systems [3].

In these pioneer experiences only the steel components of the structure were considered to resist loads while the concrete encasement was functional for protection. Although these structures were not designed for seismic loads, they behaved better under strong earthquakes than pure steel structures, thus demonstrating that inadvertent composite action probably contributed to the good performance. For these reason, today, many engineers believe that composite and hybrid systems offer an economical method to develop the strength and stiffness required for seismic design, and many systems have been developed [4] such as unbraced moment frames consisting of steel girders with concrete-filled steel tube (CFT), steel reinforced concrete (i.e. encased steel section) beam-columns, braced frames having concrete-filled steel tube columns and a variety of composite and hybrid wall systems [4]. Several research were also carried out in order to evaluate the dissipative capacity of composite structures [5] [6].

Within the European project INNO-HYCO (INNOvative HYbrid and COmposite steel-concrete structural solutions for building in seismic area) [1], funded by the Research Fund for Coal and Steel (RFCS), steel-concrete hybrid systems obtained by coupling reinforced concrete elements (e.g., walls and shear panels) with steel elements (e.g., beams) were studied. These systems permit to exploit i) the stiffness of reinforced concrete elements, necessary to limit building damage under low-intensity earthquakes, and ii) the ductility of steel elements.

In particular, in the present paper, the attention is focused on the innovative hybrid coupled shear wall (HCSW) systems, obtained coupling an RC wall with two side steel columns by means of steel links where the energy dissipation takes place.

In the following paragraphs, a general description of the solution studied, the experimental campaign on the dissipative element and connection and the results obtained are presented. A component-based model of the concrete-to-column link is then proposed, each component calibrated and the numerical results compared to the experimental ones. The present paper is based upon the work of Manfredi et al. [2], but it includes also a more detailed description of the methodology adopted and of the component model developed.

2 INNOVATIVE HYBRID COUPLED SHEAR WALL SYSTEMS

Generally, hybrid systems may suffer from some drawbacks distinctive of concrete walls and steel frames. In fact, shear walls are low redundant structures; their post-yielding behavior is characterized by deformations localized at the base and expensive detailing is required to avoid concrete crushing. Moreover, due to the excessive overturning moment generated by seismic forces at the base of the wall, expensive foundations are often required. On the other hand, steel moment resisting frames are characterized by expensive connections and dissipative elements coincide with the gravity resisting ones, making their repair difficult after the earthquake.

For these reasons, several hybrid solutions have been studied in the last decade with the aim of overcoming these drawbacks. In figure 1, the structural scheme and a detail of the dissipative element (replaceable link beam) of the HCSW system proposed and developed within the INNO-HYCO project [1], and studied within this paper, are reported.

The system studied is composed by a seismic resistant structure, constituted by a reinforced concrete wall linked to two side columns by steel elements, and by a gravity frame. In this way, the reinforced concrete wall, thanks to its high stiffness, resists almost all the horizontal shear while the overturning moment is divided partially by the individual flexural action of the wall and partially by a couple of axial forces developed within the two side columns for the benefit of the foundation and of the flexural demand on the wall base. If correctly designed, the reinforced concrete wall should remain elastic (or undergo limited damages) while dissipation should be concentrated at the steel links (dissipative elements). For this reason and in order to allow an easy repairing, the link beams should be designed to guarantee the formation of the dissipative mechanism without involving the r.c. wall or the connection system embedded on the concrete, taking into account a suitable over-strength factor of the link elements.

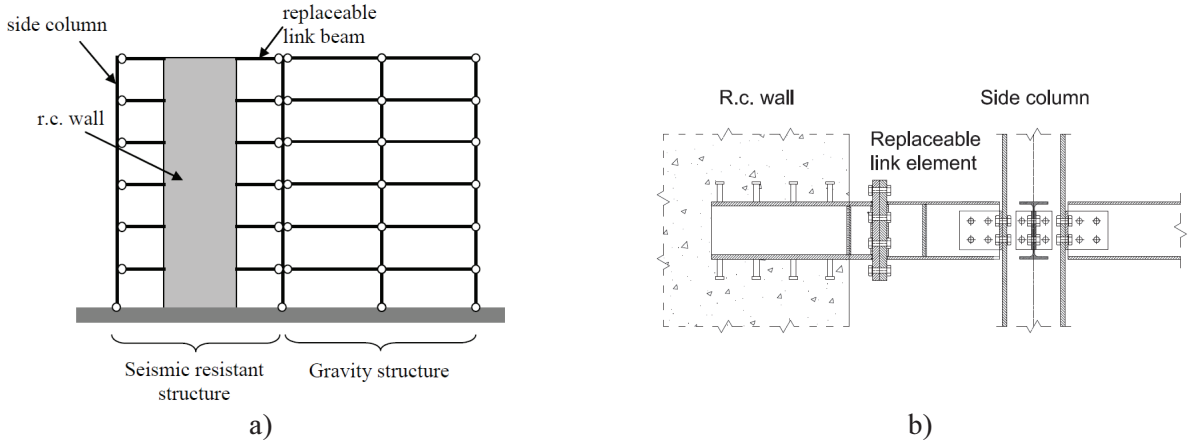

Figure 1: Innovative hybrid coupled shear wall system: a) structural scheme; b) replaceable link

A correct capacity design would allow the activation, in case of high intensity earthquakes, of a global mechanism where almost all the links would dissipate the seismic energy transmitted to the structure, containing so the forces on all the other structural elements. Such capacity design should take in particular account all the elements involved in the transmission of force from the r.c. wall to the steel column, including so the joint between wall and link and between link and steel column.

3 OBJECTIVE AND METHODOLOGY

The optimal seismic behavior of the hybrid system presented is strictly conditioned by the real behavior of the dissipative elements that, within this work, are designed to be realized by simple I profiles. Given that the hysteretic behavior and its dependence from the element mechanical and geometrical characteristics is, nowadays, well known, the main source of uncertainties is related to the characteristics of the wall-to-link and link-to-column connections. The principal objective of this article is to develop a suitable mechanical parametric model able to reproduce, in a precise and reliable manner, the cyclic behavior of the dissipative system (considering so also the presence of the connections) taking into account the influence of the mechanical and geometrical characteristics of the dissipative and connecting elements. The methodology used to develop the aforementioned mechanical model is resumed in figure 2.

In order to take into account the real hysteretic behavior of the dissipative system, an experimental campaign on two sub-systems representing two different connection typologies were carried out. For each connection typology, a total number of 5 tests were executed: 1 monotonic and 4 cyclic (2 with constant amplitude and 2 with increasing amplitude). Within this article, only the cyclic test

results were considered. The experimental behavior of the specimens allowed to select the main mechanical components that influence the global behavior of the dissipative system. Each component selected was then included in a mechanical model implemented in the OpenSEES software [7] and calibrated, in the first phase, using the experimental data and models available in the state-of-the-art literature. After a comparison between the mechanical model results and the experimental ones, a more refined calibration, using the results of the cyclic tests with increasing amplitude, was carried out allowing so to obtain a reliable mechanical model able to reproduce, in a very precise way, the experimental results obtained on the tests with constant amplitude.

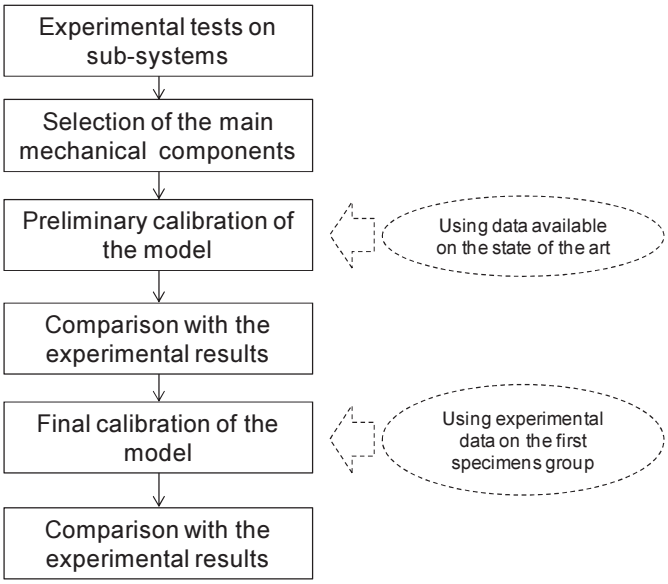

Figure 2: Methodology

4 EXPERIMENTAL CAMPAIGN

4.1 Specimens design

Within the INNO-HYCO project, 2 different case studies were designed in order to evaluate the suitable characteristics of the link element. In particular were considered a 4-storey case and a 8-storey case [1], obtaining the profile reported in table 1 for the dissipative elements.

Table 1: steel link profile (steel S355) [1]

4-storey case			8-storey case		
Floor	Link section	Link length [mm]	Floor	Link section	Link length [mm]
1st floor	IPE550	700	1st and 2nd floor	IPE550	660
2nd floor	IPE500	700	3rd and 4th floor	IPE500	660
3rd floor	IPE450	700	5th and 6th floor	IPE450	660
4th floor	IPE400	700	7th and 8th floor	IPE400	660

Starting from the obtained steel link profile obtained and considering the loading limits of the testing facility, the specimens representing the dissipative zone were downscaled. Considering an arbitrary safety factor equal to 1.5 with respect to the jack capacity, the designed intermediate link of length 660mm with section IPE500 steel S355, determined a down-scaled link with section IPE200, length equal to 360mm and steel grade S275.

Starting from the downscaled link specimens, two different typologies of link-to-wall connection have been considered: in the first case (typology 1) the bending moment is transferred by the link

to the wall primarily by the shear action of shear studs, see figure 3a; in the second case (typology 2) the moment is balanced by a couple of forces orthogonal to the embedded element axis line, see figure 3b. In both cases the configuration of the link fixed to the wall and pinned to the steel column was assumed.

Moreover, two different solutions were considered for the link splice: in one case it was placed at a distance from the concrete wall considered sufficient to allow an easy bolting of the replaceable part (solution associated to typology 1), while, in the other case, the splice connection was placed in correspondence of the face of the wall and threaded bushings were placed to allow the fasten of the link (solution associated to typology 2). Both solutions have been designed following the capacity design concept, allowing the formation of the plastic hinge on the link element without damage to the concrete wall, embedded element and joint. In both cases the link is connected to the steel column by an angle joint.

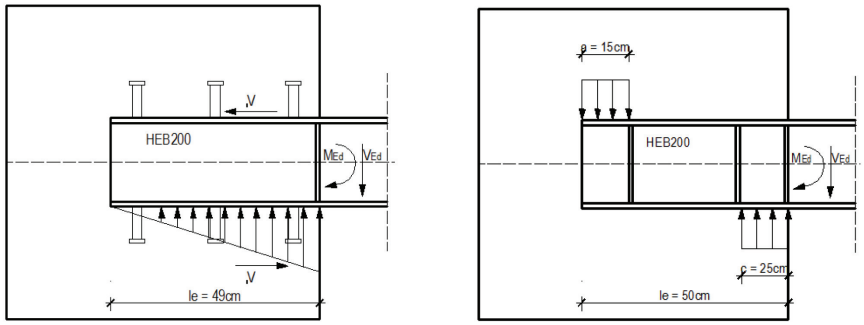

a) b)

Figure 3: Connection typology 1(a) and 2(b) [1] with the associated transmission force mechanism assumed

In figures 4 and 5, the geometrical characteristic and the realized specimens are shown. Within this paper, the experimental results and the component based model of the first connection typology is presented given that the extension to the second one is straightforward to obtain.

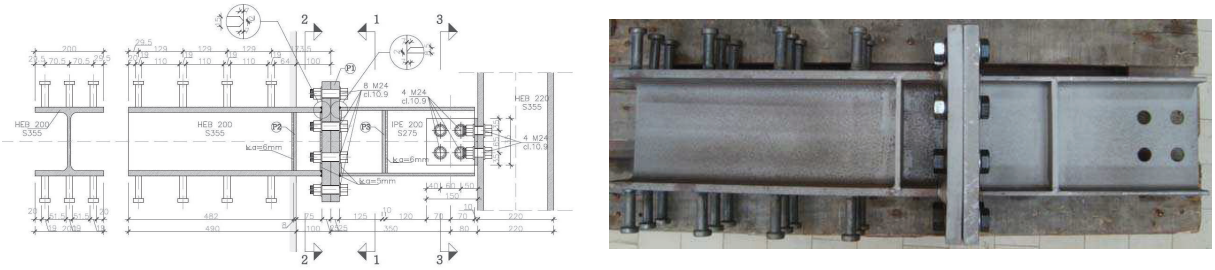

Figure 4: Connection typology 1

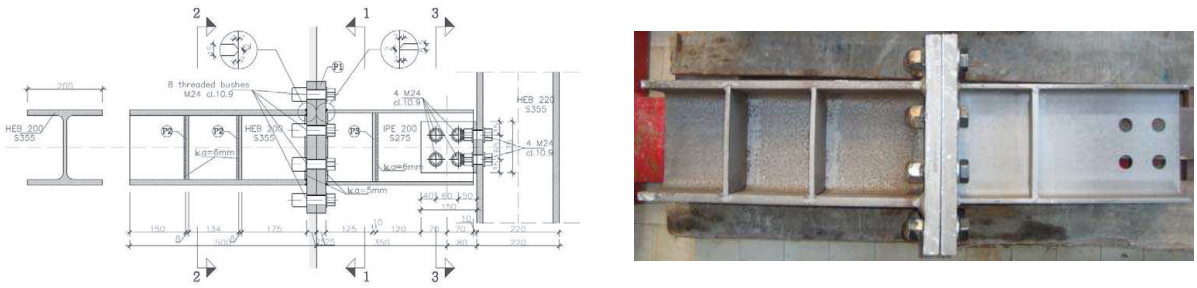

Figure 5: Connection typology 2

4.2 Test setup

In order to evaluate the behaviour of the dissipative zone as close to the real one as possible, for each connection typology, a subsystem representing the portion of the wall interested, the link-to-wall connection, the link, the link-to-column connection and the column were realized.

In figure 6, the global test setup is shown. The r.c. wall is firmly connected to the lab strong floor in order to minimize its vertical and horizontal displacement, while the shear force is transmitted to the link by an hydraulic actuator connected to the element representing the column.

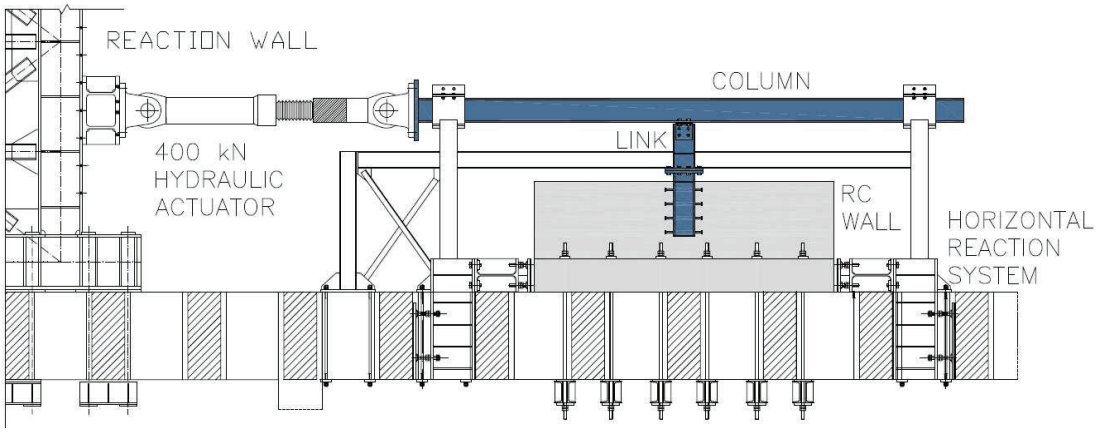

Figure 6: Global test setup

The force transmitted by the actuator was recorded by a load cell, while the displacements and the strains of the steel and concrete element by displacement sensors and strain gauges. In figure 7 the sensors position for the connection typology n°1 is shown.

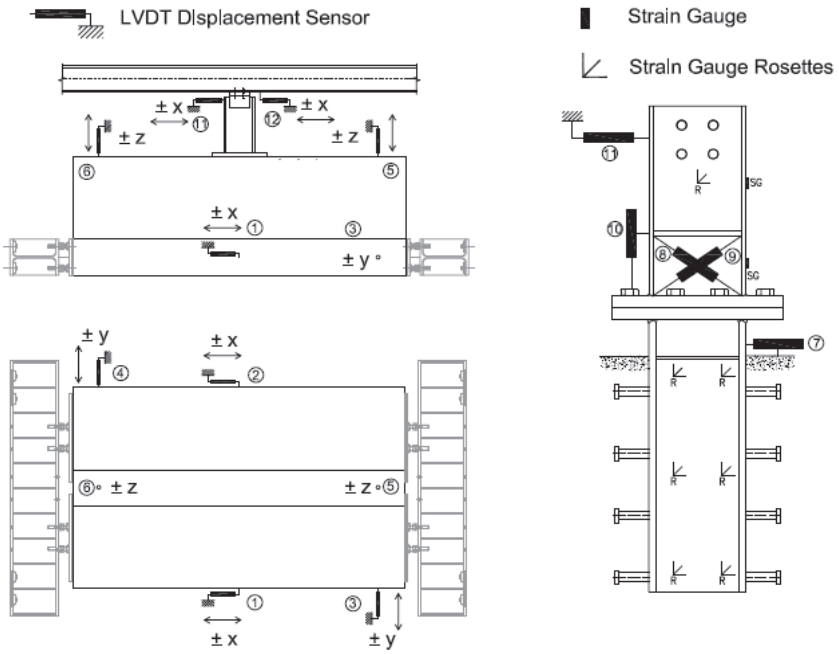

Figure 7: Sensors position

For each connection typology, 5 tests were executed, one monotonic and 4 cyclic. The first specimens couple was subjected to increasing displacement and in particular equal to 0.1 d, 0.2 d, 0.3 d, 0.5 d, 0.7d and 1.0 d (d is the displacement expected at failure). Five cycles were repeated for each intermediate step while ten cycles for the last step (1.0d). A constant amplitude, corresponding to the

design displacement d up to failure, was imposed to the second links couple with a maximum number of imposed cycles equal to 20.

4.3 Test results

In figure 8 the results of the tests, in terms of force-displacement curves, are reported. In particular, the force – link displacement (blue line) and the force – column displacement (red line) are shown.

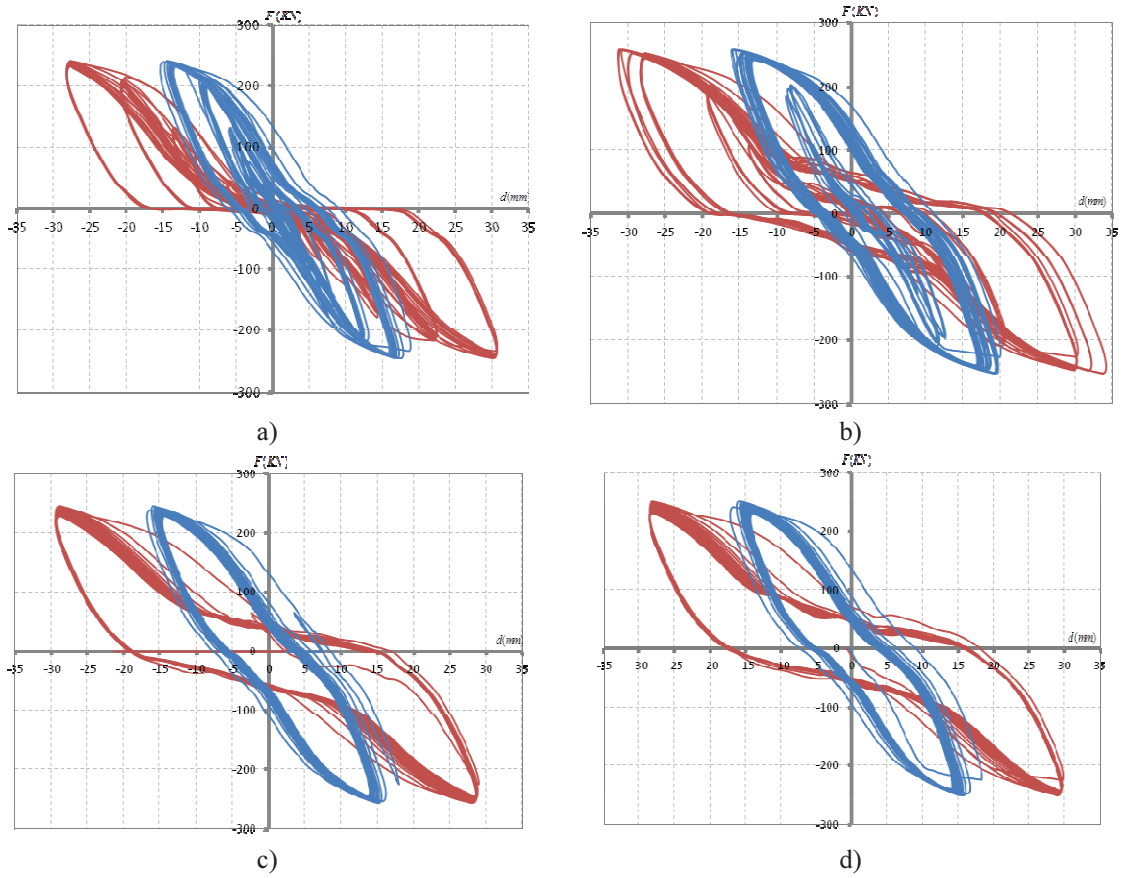

Figure 8: Force – displacement graphs with increasing amplitude (a,b) and constant amplitude (c,d) on the connection typology 1

During the first test, figure 8a, problems with the correct fastening of the bolts occurred, determining so different results from the other tests where the problem was fixed. It can be see that, while the first one is characterized by a relative "fat" hysteretic cycle, the latter one is characterized by pinching phenomena, mainly due to the gap associated to the seat joint between the link element and the column. In figure 9a, it can be seen the accentuated eccentricity of the seat angle during the test due to the gap. Moreover, the pinching phenomenon slightly increases as the maximum imposed displacement increases. In fact, due to the excessive relative rotation between the link end and the column, the link web near the seat angle plasticizes, increasing the gap between link and seat angle. In figure 9b, the ovalized holes of the link after the end of the fourth test are shown.

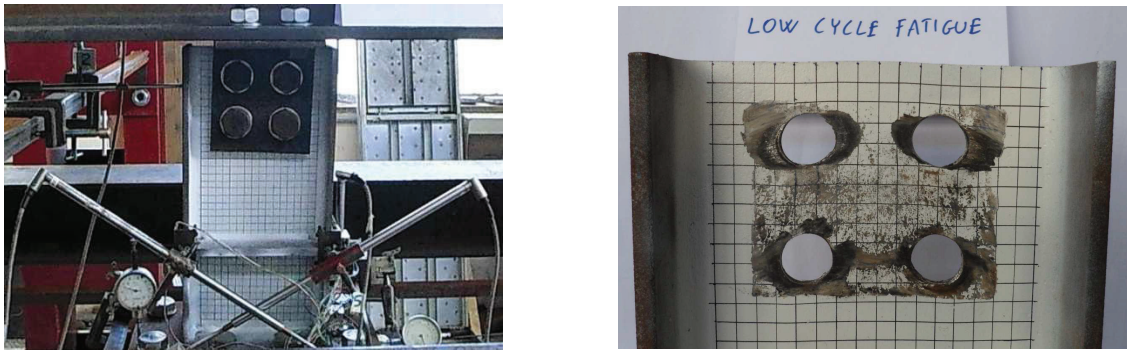

a) b)

Figure 9: a) Position of the seat angle during the test n°4; b) plasticization of the link web at the end of test n°4

In figure 10, the link force versus the relative displacement between the dissipative link and the column element relationships are shown. Two different phenomena can be individuated: 1) a linear variable friction between the angle profile and the link or column element that causes energy dissipation; 2) the pinching due to the contact and consequent ovalization of the dissipative link web holes. During the tests, no damage signs on the concrete wall were detected.

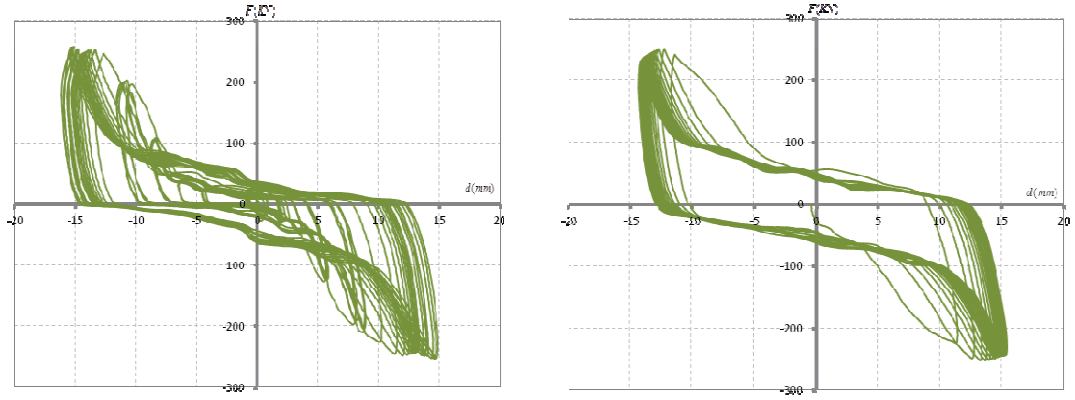

a) b)

Figure 10: Force versus link-to-column relative displacement for the test a) n° II with increasing amplitude and b) n°IV with constant amplitude.

5 COMPONENT-BASED MODEL

5.1 Definition of the model

In order to extend the experimental results obtained to joints characterized by different mechanical and geometrical characteristics and so to establish the link effective capacity to dissipate seismic energy under the action of the cyclic load, a component-based model has been developed for Connection typology 1. The model has been implemented in OpenSEES ("The Open System for Earthquake Engineering Simulation" [7]) and each component, as already specified in § 3 was calibrated, initially, using the experimental data available in the literature and compared with the experimental results obtained with the first group of specimens (tests with increasing amplitude). The global model calibration was then refined and validated using the ones of the second group (tests with constant amplitude).

Analyzing the connection configuration it is possible to subdivide it in four main zones: the embedded part, the bolted joint, the dissipative element and the connection between the dissipative element and the column.

In figure 11, the scheme of the assumed constitutive model is shown. The embedded profile, designed to remain elastic even if the dissipative element undergoes plastic deformations, was mod-

elled as an elastic beam coincident with the element axis (with reference to figure 11, element I-C). The shear studs were represented by nonlinear springs connected to the embedded element trough rigid links representing the eccentricity between the embedded profile axis and the base of the shear studs. The contact between the concrete and the embedded profile flange were modelled using unilateral extensional springs. Both the embedded element-dissipative link joint and the dissipative link-column joint were represented by rotational springs. Finally , the dissipative link was modelled using two elements: a rotational spring representing the zone where plasticization is expected and an elastic beam for the remaining zone. To each element, a suitable constitutive model was assigned and calibrated, in a first phase, on the base of the experimental results available in literature.

Embedded zone

As already mentioned, the three elements/mechanisms considered within the embedded zone were the flexural behavior HEB200 profile, the shear studs and the contact between the concrete and the steel profile flange.

The embedded element was modeled as a simple elastic beam (with reference to figure 11, element C-I). On both sides of this element were introduced 4 rigid links representing the eccentricity between the shear studs base and the HEB200 axis.

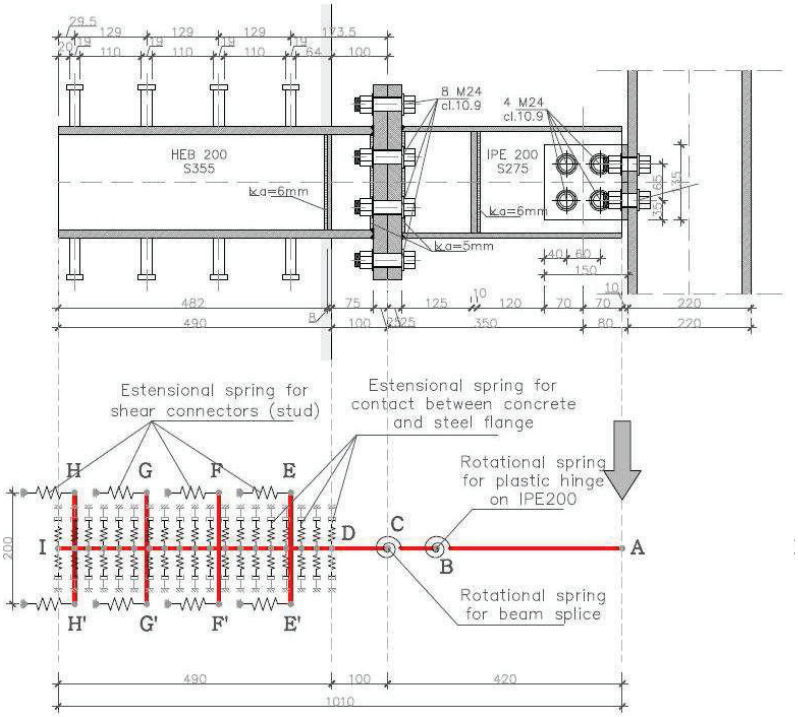

Figure 11: Constitutive model for HCSW connection typology 1

The shear studs were modeled with linear spring elements. The relation between force and slip (F-γ), for the single equivalent spring behavior formed by three connectors arranged in parallel series, was obtained processing experimental tests conducted by Aribert et al. 2000 [11]. The force-displacement relationship is schematically shown in figure 12a for the single shear stud and in figure 12b for the row composed by three shear studs.

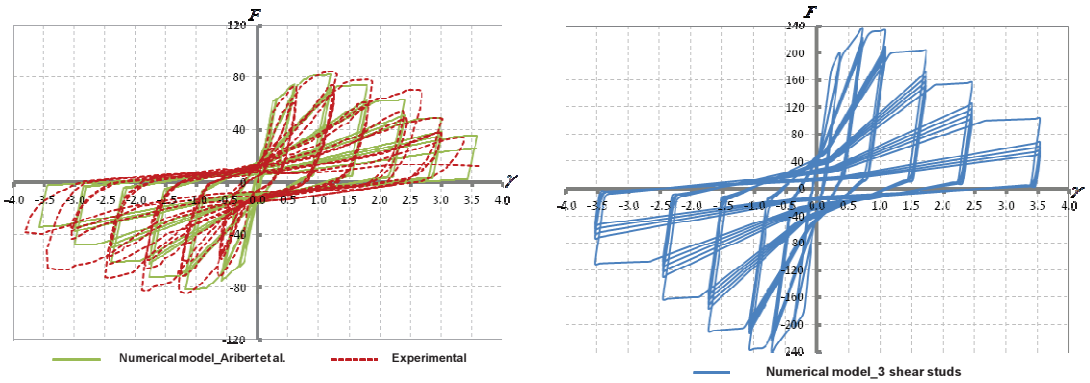

Figure 12 Force-slip relationship [11] for the a) single shear stud; b) three shear stud in a row.

Along the embedded zone, among points D-I, on the both sides of the HEB200 profile axis, a group of extensional springs placed with an inter-axis of 1cm was considered in order to represent the contact between the steel flange and the concrete wall. The concrete stress-strain relationship was evaluated in the zone comprised between the E-E' section and the I point (confined concrete) using the relation suggested by Mander et al. 1988 [12], while in the remaining zone (unconfined concrete) using the relation developed by Popovic 1973 [13], as schematically shown in figures 13 and 14. In order to take into account only the compressive reaction of the concrete, a no-tension element was associated to each spring representing the concrete. The concrete models were calibrated using the results of compression tests executed on three specimens realized with the same concrete of the r.c. wall.

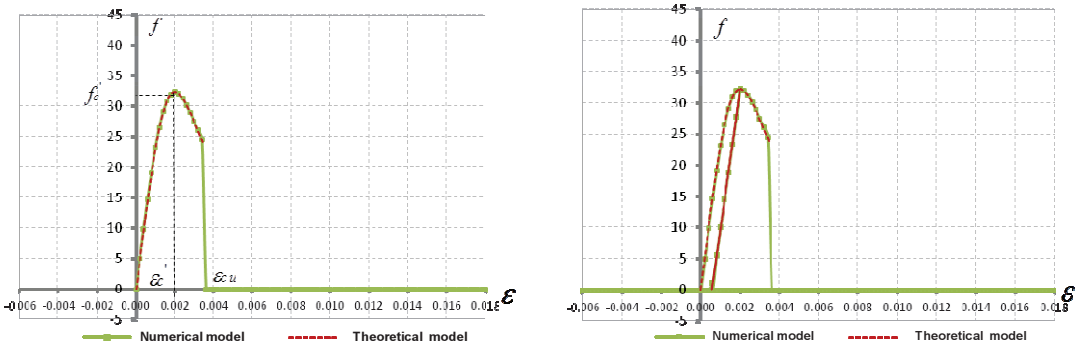

a) b)

Figure 13 Stress-strain relationship for the unconfined concrete: a) monotonic model [13]; b) cyclic model

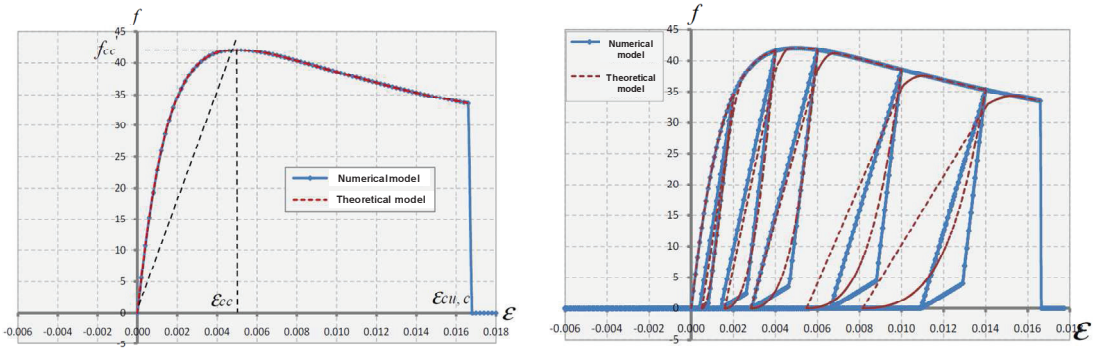

a) b)

Figure 14 Stress-strain relationship for the confined concrete [12]: a) monotonic model; b) cyclic model.

Extended end plate joint

The rotational spring placed in point C represents the flexural behavior of the beam splice and its behavior was obtained using the "Components Method" described in EN 1993-1-8:2005 [8]. The joint was originally designed as full-strength. However, in order to take into account eventual plasticization of the joint itself, the complete plastic behavior was considered. In figure 15 the theoretical behavior obtained applying the component method and the tri-linear model implemented in OpenSEES are shown. It can be seen the good approximation of the tri-linear model.

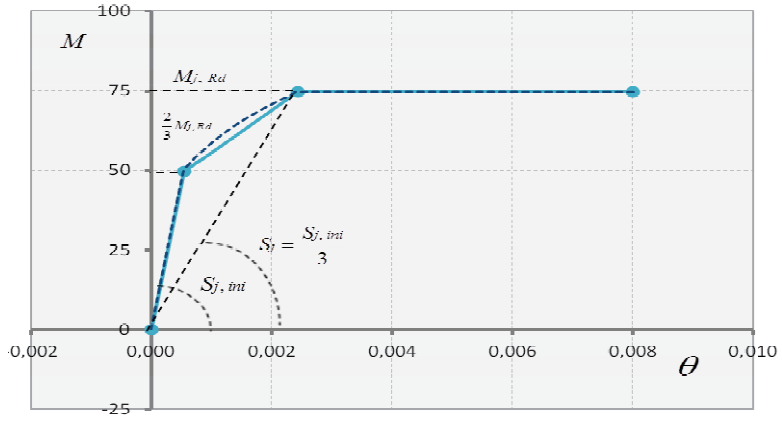

Figure 15 Moment-rotation relationship for the extended end plate joint: theoretical behavior obtained with the component method (dashed line) and numerical approximation (solid line).

Dissipative link

As already mentioned, the dissipative link was modeled using two elements: an elastic beam (element AB of figure 11) and a rotational spring (point B of figure 11) placed coincident with the center of the stiffened zone of the dissipative element. The relation between the moment and chord rotation (M-θ) was obtained processing the data of the experimental tests available on technical literature. In particular, given the lack of tests on IPE200 profiles, both the monotonic and cyclic behavior were calibrated first for an IPE300 profile and then scaled in order to obtain an estimation of the IPE200 behavior.

Both monotonic and cyclic curve for the IPE300 profile were obtained using the experimental data and the procedure described in Landolfo et al. [8].

In Landolfo et al. [8] an experimental program on a wide range of cross section typologies, comprising I sections, under monotonic and cyclic loading was carried out and a methodology for the estimation of the main parameter affecting the non-linear behavior of the section are provided. In particular, the flexural overstrength, *s*, and the rotation capacity, *R*, are evaluated through two different empirical expression, reported hereafter, functions of the geometrical and mechanical characteristics of the section.

$$1/s = C_1^{(s)} + C_2^{(s)} \cdot \lambda_f^2 + C_3^{(s)} \cdot \lambda_w^2 + C_4^{(s)} \cdot \frac{b_f}{L_v} + C_5^{(s)} \cdot \frac{E}{E_h} + C_6^{(s)} \cdot \frac{\varepsilon_h}{\varepsilon_y} \tag{1}$$

$$R = C_1^{(R)} + C_2^{(R)} \cdot \frac{1}{\lambda_f^2} + C_3^{(R)} \frac{1}{\lambda_w^2} + C_4^{(R)} \frac{b_f \cdot h}{L_v^2} + C_5^{(R)} \frac{b_f \cdot t_f}{h \cdot L_v} + C_6^{(R)} \frac{A_f}{A_{TOT}} + C_7^{(R)} \frac{L_m}{L_v} + C_8^{(R)} s \tag{2}$$

The values of the coefficients $C^{(R)}$ and $C^{(s)}$ as well as the meaning of the terms in (1) and (2) are reported in Landolfo et al [8]. Using this approach, the IPE200 monotonic and cyclic behavior was modelled in the following steps:

1) Evaluation of s_{IPE300} and R_{IPE300} for the IPE300 profile using (1) and (2)
2) Calibration of the numerical multi-linear model of the IPE300 using the experimental data available on Landolfo et al. [8].

It was assumed a multi-linear model defined using 6 points, as schematically shown in figure 16.

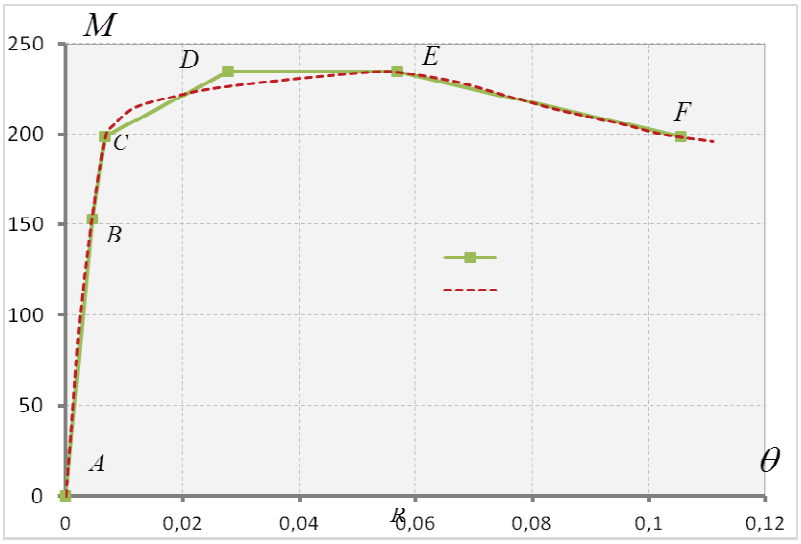

Figure 16: Moment-rotation curve for the IPE300 profile: experimental curve (dashed line) extrapolated from [8] and multi-linear model (solid line).

3) Evaluation of s_{IPE200} and R_{IPE200} for the IPE200 profile using (1) and (2)
4) Scaling of the IPE300 multi-linear curve in order to fit the IPE200 characteristics.

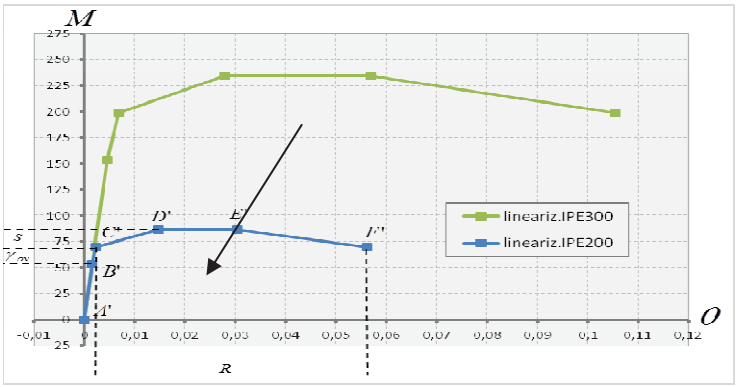

Figure 17: Moment-rotation curve for the IPE300 and IPE200 profiles

5.2 Numerical results

The comparison between the theoretical model (calibrated considering only experimental data present in literature) and the experimental results showed a good agreement in terms of strength and stiffness, but the energy dissipated by the theoretical model resulted to be higher, as schematically shown in figure 18.

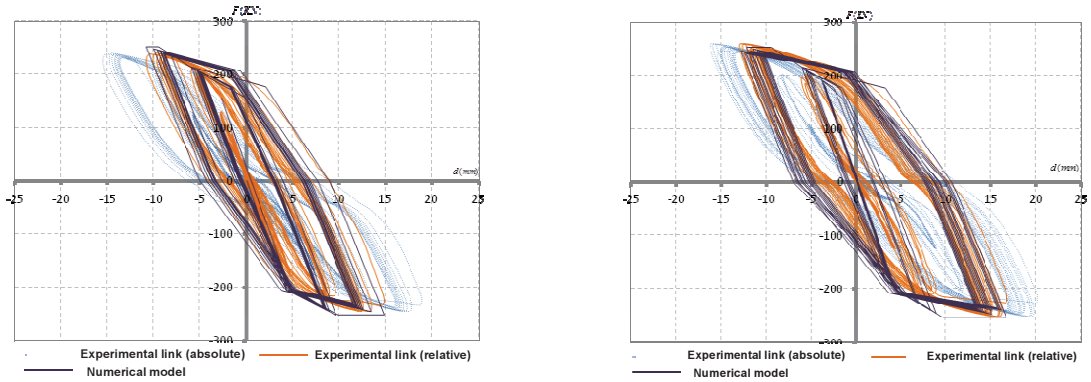

a) b)

Figure 18: comparison between the link force-displacement curve of the theoretical model (purple line) and the experimental results (orange line) of the first test group.

In order to improve the developed model, the parameter determining the stiffness degradation was calibrated using the experimental results of the first tests group (increasing amplitude). The results are shown in figures 19 and 20.

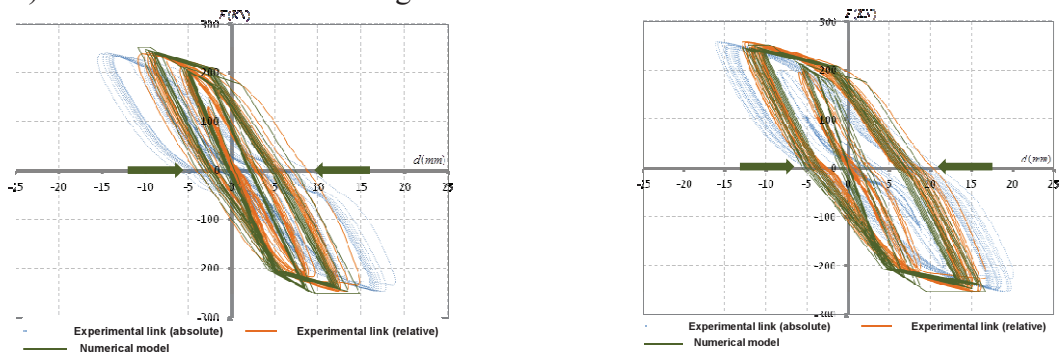

a) b)

Figure 19: comparison between the link force-displacement curve of the updated theoretical model (green line) and the experimental results (orange line) of the first test group

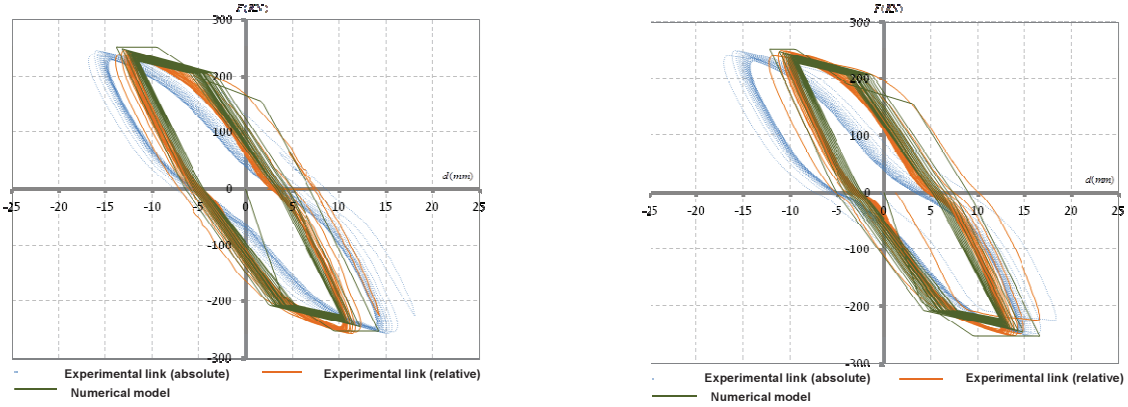

a) b)

Figure 20: comparison between the link force-displacement curve of the updated theoretical model (green line) and the experimental results (orange line) of the second test group

In figure 21 the comparison between the energy dissipated during the four tests and the numerical results obtained by the theoretical model and the calibrated one is shown. It can

be noticed that, after the calibration, the results obtained with the calibrated model are practically coincident with the experimental one even for the III° and IV° tests.

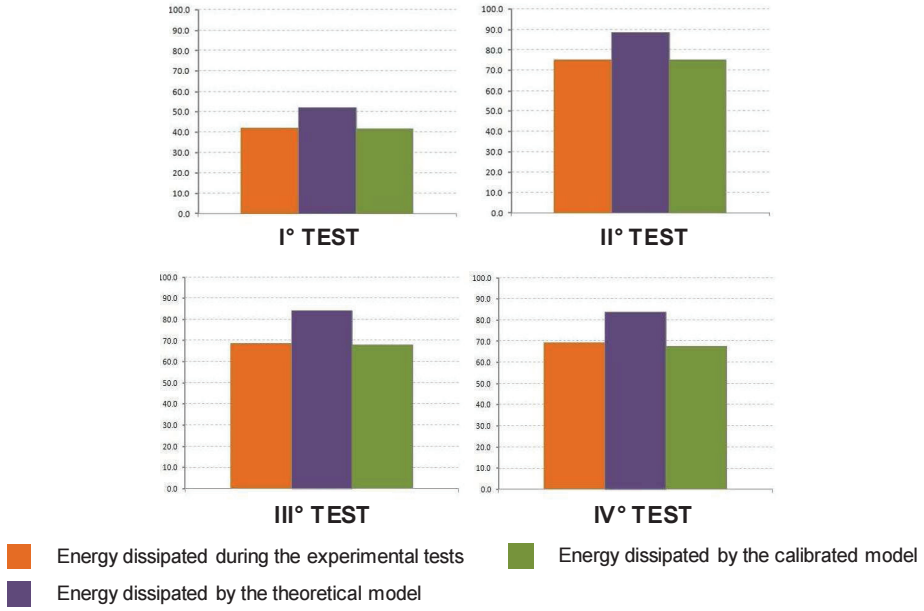

Figure 21: comparison between the energy dissipated during the four tests and the numerical results obtained by the theoretical model and the calibrated one

6 CONCLUSIONS

In the present paper, the behavior of the dissipative link of an innovative hybrid coupled shear wall systems (HCSW), obtained coupling an RC wall with two side steel columns, was studied.

The experimental results obtained from 4 downscaled specimens highlighted the good dissipative capacity of the links, but also the necessity to take into account the pinching phenomena due to the gap between the link and the column. In fact, the experimental hysteretic curves showed that the seat angle connection, commonly modelled as a perfect pin, is characterized by pinching phenomena that increases as the maximum drift increases due to the plasticization of the link web. This pinching phenomena can lead, if not correctly taken into account, to a wrong esteem of the system dissipative capacity.

Starting from the observation made during the experimental tests on 4 downscaled specimens of the dissipative link, a component-based plan model was proposed. In this first version of the model, the angle connection was not taken into account.

A first calibration of the model components was carried out using the experimental data present in literature, especially regarding the plastic hinge zone and the shear studs. From the comparison between the experimental results and the numerical ones in terms of dissipated energy, a slight adjustment of the stiffness degradation parameter was required. So, a second calibration was carried out using the experimental results of the first tests group (tests characterized by an increasing imposed amplitude). The numerical results obtained from the calibrated model were then compared to the experimental ones of the second tests group (constant imposed amplitude), showing a very good capacity of the model to predict the experimental behavior.

The obtained results permits to evaluate the dissipative behavior of the link even for different loading scenarios and set the ground for the development of a model that can take into account also the influence of the angle connection between the link and the column.

Acknowledgment

The research leading to these results has received funding from the European Union's Research Fund for Coal and Steel (RFCS) research programme under grant agreement n° [RFSR-CT-2010-00025].

References

[1] A. Dall'Asta, G. Leoni, A. Zona, B. Hoffmeister, H. Bigelow, H. Degée, C. Braham, T. Bogdan, W. Salvatore, F. Morelli, T. Prokopis, S.A. Karamanos, G. Varelis, A. Galazzi, E. Medici, P. Boni, "INNOvative HYbrid and COmposite steel-concrete structural solutions for building in seismic area – RFSR-CT-2010-00025 project – Final Report", European Commission, Brussels, 2014.

[2] M. Manfredi, F. Morelli, W. Salvatore, "Component-Based Model and Experimental Behavior of a Dissipative Steel Link for Hybrid Structures", in B.H.V. Topping, P. Iványi, (Editors), "*Proceedings of the Twelfth International Conference on Computational Structures Technology*", Civil-Comp Press, Stirlingshire, UK, Paper 165, 2014. doi:10.4203/ccp.106.165

[3] J. F. Hajjar, "Composite steel and concrete structural systems for seismic engineering", *Journal of Constructional Steel Research*, 2002.

[4] C. W. Roeder, "Overview of hybrid and composite systems for seismic design in the United States", *Engineering Structures*, 1998.

[5] A.Braconi, O.S. Bursi, G. Fabbrocino, W. Salvatore, F.Taucer, R. Tremblay "Seismic performance of a 3D full-scale high-ductility steel-concrete composite moment-resisting structure - Part II: Test results and analytical validation". *Earthquake Engineering & Structural Dynamics*, 37:1635–1655, Wiley InterScience, DOI: 10.1002/eqe.843, John Wiley & Sons, 2008

[6] A. Braconi, O. S. Bursi, G. Fabbrocino, W. Salvatore, R. Tremblay, "Seismic performance of a 3D full-scale high-ductility steel-concrete composite moment-resisting structure - Part I: Design and testing procedure", *Earthquake Engineering & Structural Dynamics*, 37:1609–1634, Wiley InterScience, DOI: 10.1002/eqe.829, John Wiley & Sons, 2008

[7] S. Mazzoni, F. McKenna, M.H. Scott, G.L.Fenves *et al.*, "Opensees Command Language Manual", 2006.

[8] M. D'Aniello, R. Landolfo, V. Piluso, G. Rizzano " Ultimate behavior of steel beams under non-uniform bending", *Journal of Constructional Steel Research*, 78, 2012.

[9] CEN (European Communities for Standardization), "EN 1993-1-8 Eurocode 3: design of steel structures -- part 8: Design of joints", 2005.

[10] A. Braconi, W. Salvatore, R. Tremblay, O.S. Bursi, "Behaviour and modelling of partial-strength beam-to-column composite joints for seismic applications", *Earthquake Engineering & Structural Dynamics*, John Wiley & Sons, 36: 142–161, 2007

[11] J. M., Aribert, O. N. Dinga, A. Lachal, "Modélisation et étude expérimentale d'assemblages de type poutre mixte-poteau en acier", *Construction Metallique*, N°1, 2000.

[12] J.B. Mander, M.J.N. Priestley, R. Park, "Theoretical Stress-Strain Model for Confined Concrete". *Journal of Structural Engineering*, Vol. 114, n°8, pagg. 1804-1825, 1988.

[13] S. Popovic, "A numerical approach to the complete stress-strain curves for concrete". *Cement and Concr. Res*., Vol. 3, n°5, pagg. 583-599, 1973.